A Scenario-Oriented Approach to Energy-Reserve Joint Procurement and Pricing

Jiantao Shi, *Student Member, IEEE*, Ye Guo, *Senior Member, IEEE*, Lang Tong, *Fellow, IEEE*, Wenchuan Wu, *Fellow, IEEE*, and Hongbin Sun, *Fellow, IEEE*

***Abstract*—We consider some crucial problems related to the secure and reliable operation of power systems with high renewable penetrations: how much reserve should we procure, how should reserve resources distribute among different locations, and how should we price reserve and charge uncertainty sources. These issues have so far been largely addressed empirically. In this paper, we first develop a scenario-oriented energy-reserve co-optimization model, which directly connects reserve procurement with possible outages and load/renewable power fluctuations without the need for empirical reserve requirements. Accordingly, reserve can be optimally procured system-wide to handle all possible future uncertainties with the minimum expected system total cost. Based on the proposed model, marginal pricing approaches are developed for energy and reserve, respectively. Locational uniform pricing is established for energy, and the similar property is also established for the combination of reserve and re-dispatch. In addition, properties of cost recovery for generators and revenue adequacy for the system operator (SO) are also proven. Simulations validate the effectiveness of the proposed mechanism.**

***Index Terms*—Electricity market, reserve, energy-reserve co-optimization, uncertainty pricing, locational marginal prices.**

I. Introduction

A. Backgrounds

THE integration of more renewable generations in power systems is an important way to achieve carbon neutrality. From 2019 to 2020, the worldwide cumulative installed capacities of solar and wind have increased by 126.74GW and 111.03GW, respectively. While in China, these two numbers are 49.25GW and 72.46GW, respectively [2], [3]. However, the increasing uncertainty brought by renewable generations also brings challenges to the secure and reliable operation of power systems. To handle this, the reserve is procured system-wide and deployed for generation re-dispatch when contingencies happen, or loads/renewable generations deviate from their predictions. Reserve and energy are strongly coupled both in generation and transmission capacity limits. A fair, efficient, and transparent energy-reserve co-optimization model and the associated market mechanism are hence of crucial importance.

B. Literature Review

Energy and reserve markets are cleared either sequentially or jointly. Currently, most of the independent system operators (ISOs) in the U.S. adopt the joint clearing process [4]–[6], stylistically defined by:

$$(\mathrm{I}): \quad \underset{\{g, r_U, r_D\}}{\text{minimize}} \quad c_g^{\mathrm{T}} g + c_U^{\mathrm{T}} r_U + c_D^{\mathrm{T}} r_D \tag{1}$$

subject to

$$(\lambda, \mu): \mathbb{1}^{\mathrm{T}} g = \mathbb{1}^{\mathrm{T}} d, S(g-d) \le f, \tag{2}$$

$$(\gamma^U, \gamma^D): \mathbb{1}^{\mathrm{T}} r_U = R^U, \mathbb{1}^{\mathrm{T}} r_D = R^D, \tag{3}$$

$$g + r_U \le \overline{G}, \underline{G} + r_D \le g, 0 \le r_U \le \overline{r_U}, 0 \le r_D \le \overline{r_D}. \tag{4}$$

The objective function (1) aims to minimize the total bid-in cost of energy g, upward reserve r_U, and downward reserve r_D. Constraints (2)-(4) represent energy balancing and transmission capacity constraints, reserve requirement constraints, and generator capacity and ramping-rate limits, respectively. Reserve clearing prices are set as the Lagrange multipliers (γ^U, γ^D), representing the marginal cost of one additional unit of upward/downward reserve requirement.

Several important issues arise from model (I). First, the reserve requirements R^U and R^D are empirical and subjective, sometimes specified as the capacity of the biggest online generator as in PJM [7] or a certain proportion of system loads as in CAISO [8]. Their values, however, can significantly affect the market clearing results and prices of both the energy and reserve products. Second, the deliverability of reserve in non-base scenarios with contingencies and load/renewable power fluctuations is not considered in (I). A common solution is to partition the entire system into different zones, each with zonal reserve requirements and prices [9], which is again ad hoc. Third,

Manuscript received 19 July 2021; revised 11 November 2021 and 21 February 2022; accepted 29 March 2022. Date of publication 7 April 2022; date of current version 22 December 2022. This work was supported by the National Natural Science Foundation of China under Grant 51977115. The work of Lang Tong was supported in part by the U.S. National Science Foundation under Award 1809830. Part of this work was presented at the 2021 IEEE PES General Meeting [1]. Paper no. TPWRS-01140-2021. *(Corresponding author: Ye Guo.)*

Jiantao Shi and Ye Guo are with the Smart Grid and Renewable Energy Laboratory, Tsinghua-Berkeley Shenzhen Institute, Shenzhen International Graduate School, Tsinghua University, Shenzhen 518071, China (e-mail: sjt21@mails.tsinghua.edu.cn; guo-ye@sz.tsinghua.edu.cn).

Wenchuan Wu and Hongbin Sun are with the State Key Laboratory of Power Systems, Department of Electrical Engineering, Tsinghua University, Beijing 100084, China, and also with the Smart Grid and Renewable Energy Laboratory, Tsinghua-Berkeley Shenzhen Institute, Shenzhen International Graduate School, Tsinghua University, Shenzhen 518071, China (e-mail: wuwench@tsinghua.edu.cn; shb@tsinghua.edu.cn).

Lang Tong is with the School of Electrical and Computer Engineering, Cornell University, Ithaca, NY 14853 USA (e-mail: lt35@cornell.edu).

Color versions of one or more figures in this article are available at https://doi.org/10.1109/TPWRS.2022.3165635.

Digital Object Identifier 10.1109/TPWRS.2022.3165635

the objective function (1) uses the base-case bid-in cost without taking into account possible re-adjustment costs. Fourth, it is not clear how the cost of procuring reserve should be afforded among all consumers. Some ISOs let all load serving entities share this cost proportionally [4], [5].

In light of these problems, many studies aim to improve the traditional model (I). For reserve requirement selection, parametric and non-parametric probabilistic forecasting techniques are incorporated in (I) by characterizing the underlying probability distribution of future situations [10]–[13]. Scenario-based approaches are also proposed in [14], [15]. In addition, on the deliverability of reserve, some statistical clustering methods are proposed in [16]–[18] that partition the network into different reserve zones. In [19], a generalized reserve disqualification approach is developed.

Stochastic co-optimization models have also been studied. In [20], a robust stochastic optimization model is adopted for the co-optimization of energy and possible re-dispatch. Moreover, the uncertainty marginal price is defined as the marginal cost of immunizing the next unit increment of the worst point in the uncertainty set. Such marginal cost is used to price both reserve resources and uncertainty sources. In [21], a chance-constrained stochastic optimization model is adopted, where statistical moments of uncertainties are considered to generate chance constraints, and an algorithm is proposed to transform the original problem to a convex formulation. In [22]–[30], the scenario-oriented stochastic optimization model structure is adopted. Some non-base scenarios with occurrence probabilities are modelled to represent possible load/renewable power fluctuations and contingencies. The energy balancing and transmission capacity constraints in all non-base scenarios are considered to analyze the re-adjustment procedures. Among those scenario-based solutions, some adopt the energy-only model structure [22]–[25]; others consider the energy-reserve co-optimization structure [26]–[30]. In [26], several possible two-stage energy and reserve pricing structures are developed and compared. In [27]–[30], locational marginal prices of energy and reserve are derived.

On the design of a pricing approach, the revenue adequacy for the SO and the cost recovery for market participants are necessary. In [22], [23], [26], both properties are established in expectation. In [24], cost recovery is established in expectation, and revenue adequacy is established for every scenario. In [25], an equilibrium model is adopted to achieve both revenue adequacy and cost recovery for each scenario with increased system costs and the reduction of social welfare.

C. Contributions, Organizations and Nomenclature

In this paper, a scenario-oriented energy-reserve joint procurement model is proposed, the associated marginal pricing approach and settlement process are developed, and many elegant market properties are established. The main contributions of this paper are listed as follows:

1) A scenario-oriented energy-reserve co-optimization model is proposed. Reserve procured from a generator is modelled as the maximum range of its power re-dispatch in all scenarios.

TABLE I
LIST OF MAJOR SYMBOLS USED

c_g, c_U, c_D:	bid-in prices of energy, upward reserve and downward reserve.
$\overline{c}, \underline{c}, c_L$:	upward/downward generation re-dispatch prices and load shedding prices.
d, π_k:	base load/load fluctuation in scenario k.
δd_k:	load shedding in scenario k.
$\delta g_k^U, \delta g_k^D$:	generation upward and downward re-dispatches in scenario k.
ϵ_k:	occurrence probability of scenario k.
η^g, η^d:	energy marginal prices of generators and loads.
η^U, η^D:	upward and downward reserve marginal prices.
f_0, f_k:	transmission capacity limit in the base case and in scenario k.
$F(\cdot)$:	objective function.
g, r_U, r_D:	generations, upward and downward reserve.
ω_0, ω_k:	base-case/non-base component of energy prices.
S, S_k:	shift factor matrices in the base case / scenario k

The proposed model no longer relies on empirical parameters of (zonal) reserve requirements. The deliverability of all reserve resources under all scenarios is ensured by incorporating the network constraints in non-base scenarios into the co-optimization model.

2) Marginal prices of energy and reserve are derived strictly following the marginal pricing principle as by-products of the co-optimization model. In addition, the associated settlement process is also developed, which includes the ex-ante settlement and the ex-post settlement after re-dispatch, and it can help to overcome the double-compensation issue in current reserve market practice. Moreover, we show that energy prices are locational uniform, and a proportional uniform pricing property can be established for reserve and re-dispatch.

3) Cost recovery for generators is established for every scenario, and revenue adequacy for the system operator is established in expectation. We show that revenue from load payments, credits to generators including energy, reserve, and re-dispatch, and congestion rent will reach their balance for both the base case and each non-base scenario.

Compared with other existing scenario-based works [22]–[30], the advantages of the proposed method are summarized as follows:

1) For those scenario-based works with an energy-only model [22]–[25], they can solve the dispatch problem of the reserve by incorporating the reserve capacity bids and several additional constraints into their models [23]. However, they do not consider the pricing problem of the reserve. In our paper, the proposed method can solve the dispatch problem and the pricing problem of reserve simultaneously.

For [26]–[30] and other existing energy-reserve co-optimization works, to the best of our knowledge, they do not focus on the ex-post settlement for the generation re-dispatch (reserve deployment) and market properties as developed in this paper. In [27]–[30], the ex-post settlement is not considered, and market property issues are not discussed. Paper [26] establishes revenue adequacy for the SO and cost recovery for generators

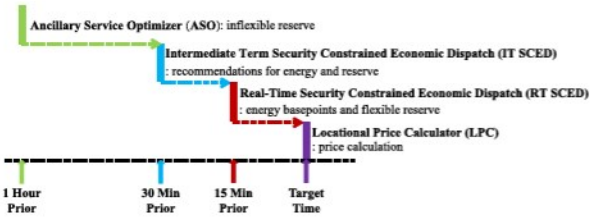

Fig. 1. PJM real-time schedules of operation reserve including ASO, IT SCED, RT SCED and LPC [7].

both in expectation, while the proposed method can establish revenue adequacy for the SO in expectation and cost recovery for generators for each scenario.

The rest of this paper is organized as follows. The proposed model is formulated in Section II. The pricing approach and the settlement process are presented in Section III. Some properties are established in Section IV. Some of the assumptions and settings are further discussed in Section V. Case studies are presented in Section VI. Section VII concludes this paper. Major designated symbols are listed in Table I.

II. Model Formulation

We consider a scenario-oriented co-optimization model. In the current market design, with PJM as an example, the reserve market consists of several look-ahead stages to procure reserve resources with different flexibility levels as shown in Fig. 1. We abstract the real-time operations in Fig. 1 into a look-ahead energy-reserve co-optimization model with the following assumptions:

i) A shift factor-based lossless DCOPF model with linear cost functions for energy and reserve is adopted, which is consistent with the current electricity market design.

ii) A single-period problem is considered for simplicity.

iii) Renewable generations are modelled as negative loads.

iv) Non-base scenarios may have line outages, load or renewable power fluctuations, etc. Generator outages, however, are not considered.

v) The objective of the proposed model is to guard against a set of mutually exclusive non-base scenarios in addition to the base case (assuming the probability of each scenario is given).

We will have further discussions on all assumptions in Section V.

Based on assumptions (i)-(v), the proposed co-optimization model is given by:

$$F(g, r_U, r_D, \delta g_k^U, \delta g_k^D, \delta d_k) = c_g^{\mathrm{T}} g + c_U^{\mathrm{T}} r_U + c_D^{\mathrm{T}} r_D + \sum_{k\in\mathcal{K}} \epsilon_k (\overline{c}^{\mathrm{T}} \delta g_k^U - \underline{c}^{\mathrm{T}} \delta g_k^D + c_L^{\mathrm{T}} \delta d_k), \tag{5}$$

$$(\mathrm{II}): \quad \underset{\{g, r_U, r_D, \delta g_k^U, \delta g_k^D, \delta d_k\}}{\text{minimize}} \; F(\cdot),$$

subject to

$$(\lambda, \mu): \mathbb{1}^{\mathrm{T}} g = \mathbb{1}^{\mathrm{T}} d, S_G \cdot g - S_D \cdot d \le f, \tag{6}$$

$$(\underline{v}, \overline{v}): \underline{G} + r_D \le g, g + r_U \le \overline{G}, \tag{7}$$

$$(\underline{\rho^U}, \overline{\rho^U}, \underline{\rho^D}, \overline{\rho^D}): 0 \le r_U \le \overline{r_U}, 0 \le r_D \le \overline{r_D}, \tag{8}$$

for all $k \in \mathcal{K}$:

$$\lambda_k: \mathbb{1}^{\mathrm{T}}(g + \delta g_k^U - \delta g_k^D) = \mathbb{1}^{\mathrm{T}}(d + \pi_k - \delta d_k), \tag{9}$$

$$\mu_k: S_{G,k}(g + \delta g_k^U - \delta g_k^D) - S_{D,k}(d + \pi_k - \delta d_k) \le f_k, \tag{10}$$

$$(\underline{\alpha_k}, \overline{\alpha_k}): 0 \le \delta g_k^U \le r_U, \tag{11}$$

$$(\underline{\beta_k}, \overline{\beta_k}): 0 \le \delta g_k^D \le r_D, \tag{12}$$

$$(\underline{\tau_k}, \overline{\tau_k}): 0 \le \delta d_k \le d + \pi_k, \tag{13}$$

where the objective function (5) is the expected system total cost, including the base-case bid-in cost as in (1) and the expectation of re-adjustment costs in all scenarios.[1] If one generator's downward reserve is deployed, its output will decrease, so will its generation cost. Therefore, there is a negative sign before the term $(\underline{c}^{\mathrm{T}} \delta g_k^D)$ in (5). Constraints (6)-(8) are base-case constraints in the same form as (2)-(4) in model (I), except for the shift factor matrices used in network constraints. The two matrices, S_G and S_D, are shift factor matrices associated with generators and loads, respectively. Constraints (9)-(10) are the energy balancing constraints and transmission capacity limits in all non-base scenarios. Note that transmission capacities in non-base scenarios f_k may not be the same as the base-case f. The impact of line outages on network topology is reflected in $S_{G,k}$ and $S_{D,k}$ compared with the base-case S_G and S_D. Constraints (11)-(12) indicate that the procured reserve will be modelled as the maximum range of generation re-dispatches in all scenarios. In constraints (9)-(10) and (13), π_k is the vector of load fluctuation parameter in non-base scenario k forecast by the SO. Therefore, constraint (13) represents that load shedding in each scenario k must be non-negative and cannot exceed load power $d + \pi_k$ in that scenario.[2]

In some market implementations, the one-step ramping constraint from the previous dispatch set point is considered as $g^{SE} - \overline{r_D} \le g \le g^{SE} + \overline{r_U}$, where g^{SE} represent actual generator outputs at the last interval from state estimation, and $\overline{r_U}, \overline{r_D}$ are the maximum upward and downward ramping rates of generators [31]. Note that this constraint can be easily incorporated into the generation capacity limit (7).

The proposed co-optimization model (II) is a standard linear programming. In this paper, we do not go into its detailed solution method, except mentioning that some distributed optimization techniques can be employed to solve it efficiently, see [32], [33].

[1] It should be noted that coefficients $\overline{c}$ and $\underline{c}$ in re-adjustment costs respectively represent the true marginal cost of upward re-dispatch and the true marginal cost reduce of generation downward re-dispatch. In some papers e.g. [23], $\overline{c}$ and $\underline{c}$ are set as the energy bid-in prices c_g. In this paper, in case some generators may incur extra costs for fast ramping, we set $\overline{c}$ and $\underline{c}$ as independent coefficients from c_g. Note that no matter how we set these two coefficients, all the qualitative analyses in this paper will always hold.

[2] We assume that δd_k and $d + \pi_k$ are non-negative. If they are negative for some resources in scenario k, it means that these resources are uncontrollable renewable generations and δd_k represents renewable curtailment. To consider this, we only need to add one more constraint $d + \pi_k \le \delta d_k \le 0$ and one associated dual variable, and all the qualitative analyses will still hold.

Moreover, from the proposed model (II) we can derive marginal prices of energy and reserve, and design the associated market settlement process, as in the next section.

III. Pricing and Settlement

A. Energy and Reserve Prices

The proposed pricing approach for energy and reserve is based on their marginal contributions to the expected system total cost in (5). Namely, consider any generator j, we first fix $g(j), r_U(j), r_D(j)$ at their optimal values $g^*(j), r_U^*(j), r_D^*(j)$ and consider them as parameters instead of decision variables. Such a modified model is referred to as model (III)

$$\underset{x_{-j}\in\mathcal{X}_{-j}}{\text{minimize}} \quad F_{-j}(x_{-j}),$$

where x_{-j} represent all the decision variables of model (II) except for $g(j), r_U(j)$ and $r_D(j)$, $F_{-j}(\cdot)$ is the overall cost excluding the bid-in cost of generator j, and $\mathcal{X}_{-j}$ are constraints (6)-(13) excluding the j^{th} row of all the constraints in (7)-(8), which are the internal constraints of generator j. Subsequently, we evaluate the sensitivity of the optimal objective function of model (III) $F_{-j}(x_{-j}^*)$, which represents the sensitivity of the expected cost of all other market participants except for generator j, with respect to parameters $g(j), r_U(j)$ and $r_D(j)$. According to the envelope theorem, the marginal energy price of generator j is

$$\begin{aligned}\eta^g(j) &= -\frac{\partial F_{-j}(x_{-j}^*)}{\partial g(j)} \\ &= \lambda^* - S_G(\cdot, m_j)^{\mathrm{T}}\mu^* + \sum_{k\in\mathcal{K}}(\lambda_k^* - S_{G,k}(\cdot, m_j)^{\mathrm{T}}\mu_k^*) \\ &= \omega_0(m_j) + \sum_{k\in\mathcal{K}}\omega_k(m_j), \end{aligned} \tag{14}$$

where m_j is the index of the bus where generator j is located. The term $(\lambda^* - S_G(\cdot, m_j)^{\mathrm{T}}\mu^*)$, denoted by $\omega_0(m_j)$, corresponds to the base-case contribution to the energy prices of generators. The term $(\lambda_k^* - S_{G,k}(\cdot, m_j)^{\mathrm{T}}\mu_k^*)$, denoted by $\omega_k(m_j)$, corresponds to the contribution to the generator energy prices of scenario k. They both follow the same form as the standard LMP, as the sum of an energy component and a congestion component.

Similarly, the energy marginal price of load l is

$$\begin{aligned}\eta^d(l) &= \frac{\partial F_{-j}(x_{-j}^*)}{\partial d(l)} = \lambda^* - S_D(\cdot, m_l)^{\mathrm{T}}\mu^* \\ &\quad + \sum_{k\in\mathcal{K}}\left(\lambda_k^* - S_{D,k}(\cdot, m_l)^{\mathrm{T}}\mu_k^* - \overline{\tau}_k^*(l)\right) \\ &= \omega_0(m_l) + \sum_{k\in\mathcal{K}}\omega_k(m_l) - \sum_{k\in\mathcal{K}}\overline{\tau}_k^*(l), \end{aligned} \tag{15}$$

which is consistent with the generator energy marginal price in (14) except for the last term $(-\sum\overline{\tau}_k^*(l))$. Here $\sum\overline{\tau}_k^*(l)$ are the multipliers associated with the upper bound limits of load shedding in (13). $\overline{\tau}_k^*(l)$ is non-zero only if load l will be totally shed in scenario k. If a load is completely shed for a particular customer whereas other loads are not, then in fact these consumers have different reliability priorities. In other words, electricity is no longer a homogeneous good for all customers. Such cases rarely happen in general.

Although the energy prices of generators and loads are defined separately in (14) and (15) at the resource level, the property of locational uniform pricing can be established for energy with an additional condition as follows:

Theorem 1 (Locational Uniform Pricing for Energy): Consider any two generators i, j and any load l at the same bus, i.e., $m_i = m_j = m_l$. Under assumptions (i)-(v) and that $\sum\overline{\tau}_k^*(l)$ is zero in (15), they have the same energy price, i.e., $\eta^g(i) = \eta^g(j) = \eta^d(l)$.

Furthermore, for the upward reserve marginal price, according to the envelop theorem, there is

$$\eta^U(j) = -\frac{\partial F_{-j}(x_{-j}^*)}{\partial r_U(j)} = \sum_{k\in\mathcal{K}}\overline{\alpha_k}^*(j). \tag{16}$$

From (16) we can see that for each generator j, if its upward generation re-dispatch reaches its procured reserve in scenario k, i.e., $\delta g_k^U(j) = r_U(j)$, then the corresponding multiplier $\overline{\alpha_k}^*(j)$ may be positive and contribute to its upward reserve marginal price $\eta^U(j)$. The upward reserve marginal price in (16) is discriminatory because reserve capacities procured from different generators at the same bus may not be homogeneous good due to their possible different re-dispatch prices.

Similarly, the downward reserve marginal price is

$$\eta^D(j) = \sum_{k\in\mathcal{K}}\overline{\beta_k}^*(j), \tag{17}$$

which is also discriminatory.

Based on the proposed pricing approach, the market settlement process will be presented in the next subsection.

B. Market Settlement Process

The proposed settlement process includes two stages: in the ex-ante stage, without knowing which scenario will happen, we solve the co-optimization problem (II) to guard against all possible non-base scenarios; and in the ex-post stage, with the realization of one specific scenario, re-adjustment strategies will be deployed according to the results from model (II), and the ex-post settlement depends on the realized scenario.

1) Ex-Ante Stage: Settlement in the ex-ante stage includes the following credits and payments:

- Base-case contribution to generator j's energy credit:

$$\Gamma_0^g(j) = \omega_0(m_j)g(j); \tag{18}$$

- Non-base contributions to generator j's energy credit:

$$\sum_{k\in\mathcal{K}}\Gamma_k^g(j) = \sum_{k\in\mathcal{K}}\omega_k(m_j)g(j); \tag{19}$$

- Base-case contribution to load l's energy payment:

$$\Gamma_0^d(l) = \omega_0(m_l)d(l); \tag{20}$$

- Non-base contributions to load l's energy payment:

$$\sum_{k\in\mathcal{K}}\Gamma_k^d(l) = \sum_{k\in\mathcal{K}}\omega_k(m_l)d(l); \tag{21}$$

- Load l's fluctuation payment, assuming $\sum \overline{\tau}_k^*(l)$ to be zero in (15):

$$\sum_{k\in\mathcal{K}} \Gamma_k^{\pi}(l) = \sum_{k\in\mathcal{K}} \frac{\partial F_{-j}(x_{-j}^*)}{\partial \pi_k(l)} \pi_k(l) = \sum_{k\in\mathcal{K}} \omega_k(m_l)\pi_k(l), \tag{22}$$

  which is contributed from its possible load fluctuations in all non-base scenarios;
- generator j's upward and downward reserve credit:

$$\Gamma^U(j) = \eta^U(j) r_U(j) = \sum_{k\in\mathcal{K}} \overline{\alpha_k}^*(j) r_U(j) = \sum_{k\in\mathcal{K}} \Gamma_k^U(j), \tag{23}$$

$$\Gamma^D(j) = \eta^D(j) r_D(j) = \sum_{k\in\mathcal{K}} \overline{\beta_k}^*(j) r_D(j) = \sum_{k\in\mathcal{K}} \Gamma_k^D(j). \tag{24}$$

Remark 1: The co-optimization model (II) is proposed to guard against all possible non-base scenarios. Although only one scenario will be realized, other ones have also contributed to the cost of procuring reserve. How to properly distribute the cost of guarding against scenarios that do not actually materialize is thus a key issue. In the proposed settlement process, consumers pay for their possible fluctuations in all non-base scenarios as in (22).

An alternative is letting consumers pay only for their actual fluctuations in the realized scenario. In this case, the fluctuation payment is ex-post and formulated as

$$\Gamma_k^{\pi}(l) = \frac{\omega_k(m_l)}{\epsilon_k} \pi_k(l), \tag{25}$$

and the SO will afford the cost of other hypothetical scenarios. As shown in [23] and in this paper, both approaches can achieve the revenue adequacy for the SO in expectation. However, we argue that load payments and the merchandise surplus of the SO are much more volatile in the approach in (25). The reason is that the reserve cost in the co-optimization model (II) mainly comes from some severe but rare scenarios. In most cases where these extreme scenarios are not realized, the load payment will be relatively low, and the net revenue of the SO will be negative. However, if one of the extreme scenarios happens, load payment will increase significantly, leading to large amounts of the SO's net revenue that can offset negative values in normal scenarios. Such drastic increases in load payment under rare but extreme scenarios, however, are sometimes unacceptable, as in the Texas power crisis in early 2021. This is an important reason for us to adopt the ex-ante settlement for possible load fluctuations. Simulations in Section VI also verify our intuitions above.

2) Ex-Post Stage: In this stage, if the base case happens, no adjustment is needed. Otherwise, assume non-base scenario k happens, then the generation re-dispatch of each generator j will be either $\delta g_k^U(j)$ or $\delta g_k^D(j)$ and will be settled with re-dispatch prices $\overline{c}$ and $\underline{c}$. Load shedding will be settled with shedding prices c_L. Therefore, the ex-post stage includes the following payments:

- upward re-dispatch credit:

$$\Phi_k^U(j) = \overline{c}(j)\delta g_k^U(j); \tag{26}$$

- downward re-dispatch pay-back:

$$\Phi_k^D(j) = -\underline{c}(j)\delta g_k^D(j); \tag{27}$$

- load shedding compensation:

$$\Phi_k^d(l) = c_L(l)\delta d_k(l). \tag{28}$$

It should be noted that with the above settlement mechanism, the realized generation re-dispatch will be settled with re-dispatch prices in (5) instead of energy marginal prices, which makes the ex-post settlement pay-as-bid. This is quite different from current reserve market practice, where the realized generation re-dispatch will be settled at the real-time energy prices plus some premiums or adders, e.g., in ERCOT [34]. The problem with these re-dispatch settlements is the false opportunity cost payment. Namely, when one generator's reserve is procured, its reserve marginal price already includes its opportunity cost in the energy market. However, if its procured reserve is deployed as generation re-dispatch in real-time operation, this generator will still receive energy credit for its re-dispatch under these re-dispatch settlements. This double-compensation problem has been mentioned by CAISO in one of its official document [35], and it can be properly addressed by adopting the proposed pay-as-bid re-dispatch settlement.

With the proposed model, the pricing approach and the settlement process, some attractive properties can be established, as in the next section.

IV. Properties

In this section, we investigate several key properties of the proposed co-optimization and pricing scheme: proportional uniform pricing for re-dispatch, individual rationality, cost recovery for generators for each scenario, and revenue adequacy for the system operator in expectation.

A. Proportional Uniform Pricing for Re-Dispatch

In the proposed settlement process, the revenue of a generator consists of three parts: (i) the ex-ante energy credit in (18) and (19), (ii) the ex-ante upward reserve credit in (23) and downward reserve credit in (24), and (iii) the ex-post upward re-dispatch credit in (26) and downward re-dispatch pay-back in (27). With Theorem 1 in Section III, the property of locational uniform pricing has been established for the generator energy credit. Next we consider establishing this property for the second and third part of generator credit as a whole. For simplicity, we only analyze the upward reserve and re-dispatch credit in this subsection, and the analysis can be easily applied to downward reserve and re-dispatch.

Note that the generator reserve revenue in (23) and the expectation of the generator re-dispatch credit in (26) can be written in a scenario-wise form as follows:

$$\sum_{k\in\mathcal{K}} (\Gamma_k^U(j) + \epsilon_k \Phi_k^U(j)) = \sum_{k\in\mathcal{K}} \Pi_k^U(j). \tag{29}$$

Each term $\Pi_k^U(j)$ in (29) can be interpreted as the fractional contribution of scenario k to the reserve and expected re-dispatch revenue of generator j. Next, we show that such fractional

revenues of different generators in the same scenario k are proportional to their re-dispatch quantities, which are referred to as the proportional locational uniform pricing property in this paper:

Theorem 2 (Proportional Uniform Pricing for Re-dispatch): For any given scenario k, consider any two generators i, j at the same bus. Under assumptions (i)-(v) and that $\delta g_k^U(i), \delta g_k^U(j) > 0$,

$$\frac{\Pi_k^U(i)}{\delta g_k^U(i)} = \frac{\Pi_k^U(j)}{\delta g_k^U(j)} = \omega_k(m_i) = \omega_k(m_j), \forall k \in \mathcal{K}. \quad (30)$$

Please check the Appendix A for the proof. Note that neither the reserve revenue in (23) nor the re-dispatch credit in (26) alone has a similar uniform pricing property. Essentially, the property of uniform pricing is a result of "the law of one price": Under certain conditions, identical goods should have the same price. However, reserve procured from different generators at the same bus may not be identical due to their different re-dispatch costs. Such a property is only true if we consider the entire re-dispatch process (23) and (26) as a whole.

B. Cost Recovery

We review properties of market participants in the proposed co-optimization model and pricing mechanism. First, we establish the property of individual rationality as the following:

Theorem 3 (Individual Rationality): Under assumptions (i)-(v) and that the lower bound of each generator's energy output $\underline{G}$ is zero, consider any generator j. We assume that its procured quantities of energy and reserve $(g^*(j), r_U^*(j), r_D^*(j))$ are solved from model (II) and its settlement prices for energy and reserve $(\eta^g(j), \eta^U(j), \eta^D(j))$ are calculated by (14), (16) and (17), respectively. Then

$$\begin{aligned} &g^*(j), r_U^*(j), r_D^*(j) \\ &= \underset{\{g(j), r_U(j), r_D(j)\}}{\operatorname{argmax}} \{F_j^{IV}(g(j), r_U(j), r_D(j)) | (7), (8)\}, \end{aligned} \quad (31)$$

where

$$\begin{aligned} F_j^{IV}(g(j), r_U(j), r_D(j)) = &\eta^g(j)g(j) + \eta^U(j)r_U(j) \\ &+ \eta^D(j)r_D(j) - c_g(j)g(j) \\ &- c_U(j)r_U(j) - c_D(j)r_D(j). \end{aligned} \quad (32)$$

In other words, if generator j were able to freely adjust its supply of energy and reserve with given prices $(\eta^g(j), \eta^U(j), \eta^D(j))$, then the solution $(g^*(j), r_U^*(j), r_D^*(j))$ to the co-optimization model (II) would have been maximized its profit.

Please check the Appendix B for the proof. Although Theorem 3 is established for the ex-ante stage only, it is still valid considering the ex-post stage. This is because the ex-post settlement is true-cost based and will not affect the profit of generators.

A natural corollary of Theorem 3 is the property of cost recovery for generators:

Corollary 1 (Cost Recovery): Under assumptions (i)-(v) and that the lower bound of each generator's energy output $\underline{G}$ is zero, with the realization of any scenario, the total credit of any generator j is no less than its total bid-in cost of energy, reserve, and re-dispatch, i.e.,

$$\begin{aligned} &\eta^g(j)g(j) + \eta^U(j)r_U(j) + \eta^D(j)r_D(j) \\ &\geq c_g(j)g(j) + c_U(j)r_U(j) + c_D(j)r_D(j). \end{aligned} \quad (33)$$

The properties of individual rationality and cost recovery for generators are established from the perspective of market participants. Next we will take the system operator's point of view and establish the revenue adequacy property.

C. Revenue Adequacy

For the SO, its total congestion rent Δ from the proposed model (II) is the sum of the contribution Δ_0 from the base case and the contributions $\sum_{k \in \mathcal{K}} \Delta_k$ from all non-base scenarios. Δ_0 and Δ_k are calculated by the following equations:

$$\Delta_0 = f^{\mathrm{T}} \mu^*, \quad (34)$$

$$\Delta_k = f_k^{\mathrm{T}} \mu_k^*. \quad (35)$$

For the proposed settlement process, the following property regarding the SO's revenue adequacy can be established:

Theorem 4 (Revenue Adequacy): Under assumptions (i)-(v) and that $\sum \overline{\tau}_k^*(l)$ is zero in (15), in expectation, total load payment is equal to the sum of total generator credit and total congestion rent Δ.

Moreover, the property of revenue adequacy can be decomposed scenario-wise. Namely, the base-case load energy payment (20) is equal to the sum of the base-case generator energy credit (18) and the base-case congestion rent (34):

$$\mathbb{1}^{\mathrm{T}} \Gamma_0^d = \mathbb{1}^{\mathrm{T}} \Gamma_0^g + \Delta_0. \quad (36)$$

And for each non-base scenario k, the sum of its contribution to load payment $\mathbb{1}^{\mathrm{T}}(\Gamma_k^d + \Gamma_k^\pi)$ in (21)-(22) is equal to the sum of its contribution to generator ex-ante energy credit $\mathbb{1}^{\mathrm{T}} \Gamma_k^g$ in (19) and reserve credit $\mathbb{1}^{\mathrm{T}}(\Gamma_k^U + \Gamma_k^D)$ in (23)-(24), the expected generator ex-post re-dispatch payment $\mathbb{1}^{\mathrm{T}}(\epsilon_k \Phi_k^U + \epsilon_k \Phi_k^D)$ in (26)-(27), the expected load shedding compensation $\mathbb{1}^{\mathrm{T}}(\epsilon_k \Phi_k^d)$ in (28), and the congestion rent Δ_k in (35):

$$\begin{aligned} &\mathbb{1}^{\mathrm{T}}(\Gamma_k^d + \Gamma_k^\pi) \\ &= \mathbb{1}^{\mathrm{T}}(\Gamma_k^g + \Gamma_k^U + \Gamma_k^D + \epsilon_k \Phi_k^U + \epsilon_k \Phi_k^D + \epsilon_k \Phi_k^d) + \Delta_k, \forall k \in \mathcal{K}. \end{aligned} \quad (37)$$

Please refer to the Appendix C for the proof. With (37), it can be observed that in expectation, ex-ante reserve procurement cost and ex-post re-adjustment cost are allocated scenario-wise to loads based on their load fluctuation severity.

V. Discussions

In this section, we revisit all assumptions and discuss their implications, as well as some extensions.

In assumption (i), we assume that a shift factor-based lossless DCOPF model with linear cost functions for energy and reserve is adopted. This assumption is standard and is consistent with the current electricity market design.

In assumption (ii), we assume that a single-period problem is considered for simplicity, whereas practical reserve markets may follow a multi-period setting. It should be noted that the proposed single-period model (II) can be easily extended into a one-shot multi-period model by incorporating the inter-temporal ramping constraints between sequential intervals, and such extension is formulated in the Appendix D. Namely, consider any generator j, assume that at period $t-1$, its energy procurement is g_{t-1} and its upward reserve procurement is $r_{U,t-1}$. During the transition from period $t-1$ to period t, generator j not only needs to ramp up its output from g_{t-1} to g_t, it also needs to keep part of its ramping rate for the provision of upward reserve $r_{U,t-1}$. Therefore, the sum of its upward ramping from period $t-1$ to period t $(g_t - g_{t-1})$ and its procured upward reserve at period $t-1$ $r_{U,t-1}$ cannot exceed the maximum upward ramping rate between sequential periods Δg^U, i.e., $g_t - g_{t-1} + r_{U,t-1} \le \Delta g^U$ as in (76). Similarly, for downward reserve and ramping, we have $-g_t + g_{t-1} + r_{D,t-1} \le \Delta g^D$ in (77). At the same time, we have also developed a multi-period extension of the proposed pricing approach and settlement process, and we have performed simulations of multi-period system operation, see [36]. Moreover, note that the biggest challenge in a multi-period problem is the coupling between reserve and ramping, which is a highly complicated issue in a look-ahead rolling-window dispatch, see [37] as an example. Since the main purpose of this paper is to focus on the reserve issue, we will leave the multi-period rolling-window dispatch problem to our future works.

In assumption (iii), we assume that renewable generations are modelled as negative loads. In essence, we assume that the system always accommodates all renewable energy available in the ex-ante energy procurement. Consequently, renewable generators will have the same effects as loads from the perspective of the co-optimization model (II). In addition, renewables can also be regarded as reserve resources with stochastic upper bounds, but this is out of the scope of this paper.

In assumption (iv), we ignore generator outages in non-base scenarios to establish the property of locational uniform pricing for energy. If generator outages are considered, the co-optimization model and prices can be obtained similarly. In particular, the objective function (5) and base-case constraints (6)-(8) will remain the same, while non-base constraints (9)-(12) will be modified as

$$\lambda_k : 1^{\mathrm{T}}(\widetilde{g}_k + \delta g_k^U - \delta g_k^D) = 1^{\mathrm{T}}(d + \pi_k - \delta d_k), \tag{38}$$

$$\mu_k : S_{G,k}^{\mathrm{T}}(\widetilde{g}_k + \delta g_k^U - \delta g_k^D) - S_{D,k}^{\mathrm{T}}(d + \pi_k - \delta d_k) \le f_k, \tag{39}$$

$$(\underline{\alpha_k}, \overline{\alpha_k}) : 0 \le \delta g_k^U \le \widetilde{r}_{U,k}, \tag{40}$$

$$(\underline{\beta_k}, \overline{\beta_k}) : 0 \le \delta g_k^D \le \widetilde{r}_{D,k}, \tag{41}$$

where $\widetilde{g}_k, \widetilde{r}_{U,k}, \widetilde{r}_{D,k}$ are the vectors of available generations and reserve capacities in scenario k considering possible generator outages in that scenario. With these modifications, the proposed co-optimization can efficiently model generator outages and optimally procure reserve to guard against them.

Moreover, considering the pricing in this case, for generator j, its energy and reserve prices in (14) and (16)-(17) will be modified as

$$\begin{aligned}\eta^g(j) &= -\frac{\partial F_{-j}(x_{-j}^*)}{\partial g(j)} = \lambda^* - S_G(\cdot, m_j)^{\mathrm{T}}\mu^* \\ &\quad + \sum_{k \in \mathcal{K}, j \notin \Omega_k} (\lambda_k^* - S_{G,k}(\cdot, m_j)^{\mathrm{T}}\mu_k^*) \\ &= \omega_0(j) + \sum_{k \in \mathcal{K}, j \notin \Omega_k} \omega_k(j),\end{aligned} \tag{42}$$

$$\eta^U(j) = -\frac{\partial F_{-j}(x_{-j}^*)}{\partial r_U(j)} = \sum_{k \in \mathcal{K}, j \notin \Omega_k} \overline{\alpha_k}^*(j), \tag{43}$$

$$\eta^D(j) = -\frac{\partial F_{-j}(x_{-j}^*)}{\partial r_D(j)} = \sum_{k \in \mathcal{K}, j \notin \Omega_k} \overline{\beta_k}^*(j), \tag{44}$$

where Ω_k is the set of generators that are shut down in scenario k. Compared with the original pricing formulations in (14) and (16)-(17), it can be observed that if generator j is shut down in scenario k, then this scenario should be excluded from the calculation of its energy and reserve prices, indicating the complicated issue of non-uniform pricing brought by generator outages. Namely, considering generators at the same bus but with different outage probabilities, they will receive different energy marginal prices because their generations are no longer homogeneous goods. Similarly, reserve capacities from these generators are not homogeneous goods either even if they have the same re-dispatch price. These complicated issues cannot be fully addressed as a part of this paper, therefore more efforts will be made to them in our future studies.

In assumption (v), we assume that the probability of each scenario is a given parameter, and we did not address how such a parameter can be estimated and the costs of inaccurate parameter estimation in our paper. This is a difficult problem in general for all scenario-based approaches. We provide an empirical evaluation of the impact of unforeseen scenarios with the outage of the biggest online generator and some load fluctuations. In particular, we study the relationship between the system regret cost and the occurrence probabilities of these unforeseen scenarios. The detailed result is presented in Section VI.B.

Some discussions on the absence of unit commitment are also in order. The proposed co-optimization model and the associated pricing approach apply primarily to the real-time (or near real-time) electricity markets (See Fig. 1), where unit commitment (UC) is rarely used. Therefore, we consider an economic dispatch (ED) problem with fixed UC decisions in this paper. This is also in line with many electricity market practices in the U.S. For example, as shown in Fig. 1, the reserve market in PJM consists of several real-time or near real-time look-ahead ED modules, while UC decisions in PJM are determined in the day-ahead market clearing [38].

VI. Case Study

Case studies were performed both on a 2-bus system and modified IEEE 118-bus system. Note that for all simulations

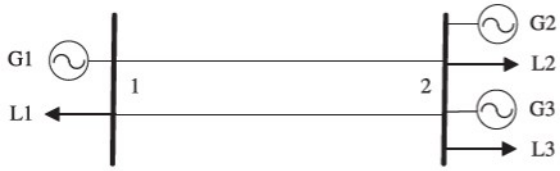

Fig. 2. One-Line Diagram of the 2-Bus System.

TABLE II
GENERATOR PARAMETERS OF THE 2-BUS CASE

Generator	$\overline{G}/\underline{G}$	$\overline{r_U}/\overline{r_D}$	$c_g/c_U/c_D$
G1	16/0	4/4	8/2/2
G2	18/0	4/4	15/2/2
G3	12/0	4/4	20/2.5/2.5

TABLE III
NON-BASE SCENARIOS FOR THE 2-BUS CASE

NO.	Line outage	Load	Probability
1	Yes	(6,15,4)	0.06
2/3	Yes	(8,21,3)/(9,17,1)	0.02/0.02
4/5	No	(8,21,3)/(9,17,1)	0.18/0.18

TABLE IV
CLEARING RESULTS AND PRICES OF THE 2-BUS CASE

Generator	g	r_U	r_D	η^g	η^U	η^D
G1	8.0	2.4	0.8	8.0	2.0	2.0
G2	16.4	1.6	0.0	20.0	7.0	2.0
G3	0.6	4.0	0.4	20.0	6.0	2.5

in this section, we set re-dispatch prices $\overline{c}$ and $\underline{c}$ as the energy bid-in prices c_g, and we have quantities in MW and prices in \$/MWh. For simplicity, the units are omitted hereafter.

A. Two-Bus System

First, a simple 2-bus system was adopted to illustrate the proposed co-optimization and pricing mechanism, as well as properties thereof. The one-line diagram was presented in Fig. 2. There were two parallel and identical transmission lines, each with a capacity of 1MW. For non-base scenarios, one of the two parallel lines may be cut off. In addition, in non-base scenarios, the power flow limit on each transmission line was set as 1.2MW. Furthermore, generator parameters of this 2-bus case were presented in Table II, and the base load vector for L1, L2 and L3 was (6,15,4)MW. Moreover, all possible non-base scenarios for this 2-bus case were given in Table III, and the probability of the base case happening was $1-\sum \epsilon_k = 0.54$.

Market clearing results and prices of the 2-bus case with the proposed model (II) were presented in Table IV. For cleared quantities, note that although G1 offers the cheapest upward reserve and still has extra generation capacity and ramping rate, the SO does not clear G1's entire upward reserve. Instead, the more expensive upward reserve resources G2 and G3 are cleared. The reason is that the extra upward reserve from G1 will not be deliverable in scenarios with line outages. In addition, from the 5^{th} column of Table IV, it can be confirmed that the energy prices are locational uniform. Furthermore, from the $6^{th}-7^{th}$ columns it can be observed that G2 receives a higher upward reserve price but a lower downward reserve price compared with G3 because G2's upward and downward re-dispatch prices $\overline{c}, \underline{c}$ are both lower.

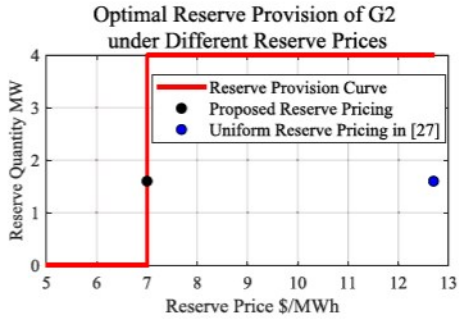

Fig. 3. Optimal Upward Reserve Provision of G2 with respect to the Increasing Upward Reserve Price from the SO.

Different from the proposed discriminative reserve pricing, in [27], while the energy pricing approach is the same as the proposed one in (14), a locational uniform reserve pricing approach is adopted. Specifically, in [27], the reserve clearing price of all generators at bus m_j is set as $\sum_{k\in\mathcal{K}} \omega_k(m_j)$, where $\omega_k(m_j)$ is the contribution to the generator energy prices of scenario k as in (14). With such a pricing formulation, the upward reserve price of G2 is 12.7 \$/MWh. To compare these two different reserve pricing methods, in this toy example, we consider the individual rationality problem of G2, whose generation upper bound constraint is binding: with different reserve price signals from the SO, the optimal reserve provision of G2 can also be different. In that sense, we inputted different reserve prices into the profit maximization model of G2 presented in (31)-(32) to calculate the optimal reserve provision of G2, and we presented the optimal reserve provision of G2 as the red curve in Fig. 3. In addition, in Fig. 3, G2's reserve clearing price-quantity pair under the proposed reserve pricing approach was presented by the black spot, and its reserve clearing price-quantity pair under the locational uniform reserve pricing approach in [27] was presented by the blue spot. The overall trend of the red curve is upward because, with a higher reserve price, G2 is willing to provide more upward reserve. In addition, it can be observed that the black dot lies on the red curve, meaning that under the proposed reserve pricing approach, the reserve clearing quantity can maximize G2's profit. On the contrary, the blue dot is not on the red curve, meaning that under the locational uniform reserve pricing in [27], the reserve clearing quantity cannot maximize G2's profit. This small case validates the advantage of the proposed reserve pricing approach over the existing locational uniform reserve pricing approach.

Moreover, the proportional locational uniform pricing property for re-dispatch was illustrated in Table V. We have $\delta g_k^U(2), \delta g_k^U(3) > 0$ for G2 and G3 in scenarios 2 and 4, and in these two scenarios we have $\frac{\Pi_k^U(2)}{\delta g_k^U(2)} = \frac{\Pi_k^U(3)}{\delta g_k^U(3)} = \omega_k(m_2) = \omega_k(m_3)$, validating Theorem 2.

TABLE V
PROPORTIONAL LOCATIONAL UNIFORM PRICING FOR RE-DISPATCH IN THE 2-BUS CASE

Scenario	Generator	δg_k^U	Π_k^U	$\frac{\Pi_k^U}{\delta g_k^U}$	ω_k
Scenario 2	G2	1.60	1.92	1.20	1.20
	G3	4.00	4.80	1.20	1.20
Scenario 4	G2	1.60	17.08	8.80	8.80
	G3	4.00	35.20	8.80	8.80

TABLE VI
MONEY FLOW IN THE 2-BUS CASE($)

	Base	S1	S2	S3	S4	S5	Total
Γ^d	482.0	8.0	23.8	6.7	187.4	37.4	745.2
Γ^π	0	0	7.5	0.2	59.5	3.0	70.2
Γ^g	476.0	3.2	21.7	6.4	176.5	37.4	721.2
Γ^U	0	0	4.6	0	35.2	0.1	40.0
Γ^D	0	1.7	0	0.1	0	0.8	2.6
$\epsilon\Phi^U$	0	1.1	2.3	0.4	22.2	3.5	29.5
$\epsilon\Phi^D$	0	−0.8	−0.1	−0.2	0	−1.4	−2.5
$\epsilon\Phi^d$	0	0	1.4	0	0	0	1.4
Δ	6.0	2.9	1.2	0.2	13.0	0	23.3

Furthermore, with the realization of any non-base scenario, profits of G1, G2 and G3 are \$101.60, \$298.28, \$21.62, respectively, which confirms the property of cost recovery. In addition, in Table VI, the money flow in this 2-bus case was presented. We can see that in expectation, payments from loads, credits to generators and congestion rent can reach their balance for the base case as in the 2^{nd} column, for each scenario as in the $3^{rd} - 7^{th}$ columns, and in total as in the last column, validating the property of revenue adequacy.

B. IEEE 118-Bus System

Simulations on modified IEEE 118-bus system were also recorded. The transmission capacities were modified as 1.5 times of the DCOPF results of the original IEEE 118-bus system. In addition, transmission capacities that were smaller than 10MW would be set as 10MW. In non-base scenarios, power flow limits on transmission lines were set as 1.3 times of the base-case values. The generation cost of each generator was modified as a linear term, and its upward and downward reserve bid-in prices were both set as 1/5 of its energy bid-in price. Moreover, the upward and downward ramping rates of each generator were both set as 0.1 times of its generation capacity upper bound. In addition, the original load 59 was equally separated into two loads: new load 59 and load 119. Furthermore, minor modifications were also applied to some load capacities. We uploaded our Matlab case file onto Github as in [39]. In addition, all possible non-base scenarios in this case were given in Table VII. In this subsection, in-sample tests were performed based on the in-sample scenarios in Table VII to illustrate properties of the proposed co-optimization and pricing. We also performed the out-of-sample test with some additional settings.

In Fig. 4, with the Monte Carlo Simulation, the average system cost of the proposed model was compared with that of the traditional model under different reserve requirement settings, with the following steps:

TABLE VII
NON-BASE SCENARIOS FOR THE 118-BUS CASE

NO.	Outage	Load Situation	Probability
1	No outage	d119 ↑ by 3%, others ↓ by 3%	0.07
2	No outage	d119 ↓ by 3%, others ↑ by 3%	0.07
3	Line 21	d119 ↑ by 3%, others ↓ by 3%	0.01
4	Line 21	d119 ↓ by 3%, others ↑ by 3%	0.01
5	Line 21	basic load	0.08
6	Line 55	d119 ↑ by 3%, others ↓ by 3%	0.01
7	Line 55	d119 ↓ by 3%, others ↑ by 3%	0.01
8	Line 55	basic load	0.08
9	Line 102	d119 ↓ by 3%, others ↑ by 3%	0.01
10	Line 102	d119 ↓ by 3%, others ↑ by 3%	0.01
11	Line 102	basic load	0.08

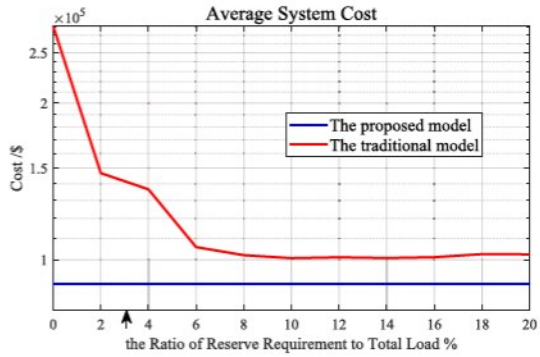

Fig. 4. Average system costs from the proposed model (blue) and the traditional model under different reserve requirement settings (red).

(i) We selected different reserve requirements as different ratios of the system total load for the traditional model;

(ii) We calculated the energy and reserve clearing results and base-case procurement costs of the modified 118-bus case with the traditional model under these different reserve requirement settings from step (i);

(iii) We generated 50000 Monte Carlo Samples based on the occurrence probabilities of non-base scenarios in Table VII;

(iv) We calculated the average re-adjustment costs of the traditional model under different reserve requirement settings in all Monte Carlo Samples. If the re-adjustment problem was infeasible in one Monte Carlo Sample, then the re-adjustment cost was set as 200000, whereas the expected system total cost from the proposed model (II) was 89651.6 in this case.

(v) We obtained the average system costs of the traditional model under different reserve requirement settings by adding the base-case procurement costs from step (ii) to the average re-adjustment costs from step (iv), and presented them in Fig. 4 as the red curve. Note that with the increasing reserve requirement, the red curve first goes down because of the decreasing load shedding cost, and it then goes up because of the increasing reserve procurement cost.

(vi) We repeated steps (ii)-(v) for the proposed model (II) and presented the average system cost of the proposed model in Fig. 4 as the blue curve. The overall upward and downward reserve procurement of the modified 118-bus case with the proposed model $\mathbb{1}^{\mathrm{T}} r_U^*$ and $\mathbb{1}^{\mathrm{T}} r_D^*$ were both about 3% of system total load, indicated by an arrow in Fig. 4. We can observe that the

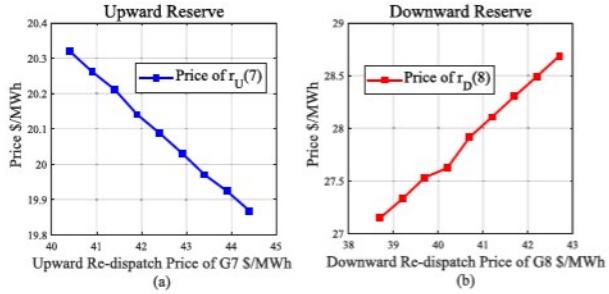

Fig. 5. (a) Price of G7's upward reserve $r_U(7)$ with respect to the increasing upward re-dispatch price of G7; (b) Price of G8's downward reserve $r_D(8)$ with respect to the increasing downward re-dispatch price of G8.

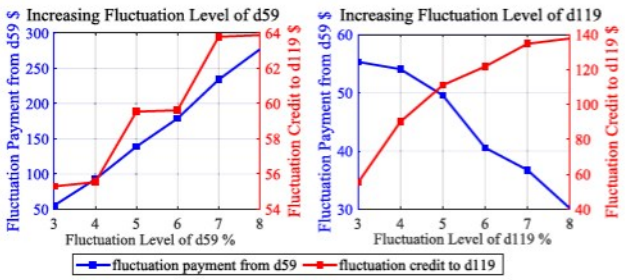

Fig. 6. (a) Fluctuation payment from d59 (blue) and fluctuation credit to d119 (red) with respect to the increasing fluctuation level of d59; (b) Fluctuation payment from d59 (blue) and fluctuation credit to d119 (red) with respect to the increasing fluctuation level of d119.

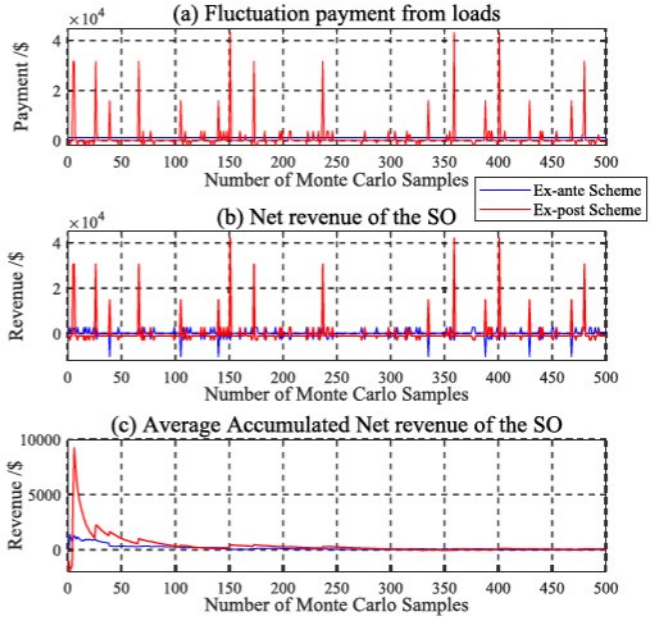

Fig. 7. (a) Fluctuation payment from loads in much Monte Carlo Samples under the ex-ante scheme (blue) and the ex-post scheme (red); (b) Net revenue of the SO in much Monte Carlo Samples under the ex-ante scheme (blue) and the ex-post scheme (red); (c) Average accumulated net revenue of the SO in much Monte Carlo Samples under the ex-ante scheme (blue) and the ex-post scheme (red).

proposed model could reduce reserve procurement and reduce the average system cost by 10.99%-68.14% in this test compared with the traditional model.

In addition, in Fig. 5, the relationships between reserve marginal prices and re-dispatch prices were presented. In Fig. 5(a), with the increasing upward re-dispatch price of G7, the upward reserve price of G7 decreases. At the same time, In Fig. 5(b), with the increasing downward re-dispatch price of G8, the downward reserve price of G8 increases because of the negative sign before the term $\underline{c}^{\mathrm{T}}\delta g_k^D$ in (5).

In addition, from Table VII, it can be observed that in non-base scenarios with load fluctuations, the fluctuation levels of all loads are 3%. We fixed the fluctuation levels of all other loads except for d59 and d119, and showed how the fluctuation payment from d59 and the fluctuation credit to d119 (the opposite of the fluctuation payment from d119) in (22) change with the increasing fluctuation level of d59 in Fig. 6(a), and how they change with the increasing fluctuation level of d119 in Fig. 6(b), where the blue curve represents the fluctuation payment from d59, and the red curve represents the fluctuation credit to d119. In both Fig. 6(a) and Fig. 6(b), the fluctuation credit to d119 is always positive because d119's fluctuation can offset the fluctuations of other loads in non-base scenarios as shown in Table VII. In Fig. 6(a), with the rising fluctuation level of d59, both the fluctuation payment from d59 and the fluctuation credit to d119 increase: For d59, its rising fluctuation level brings in more uncertainties to the system; At the same time, for d119, considering the increasing uncertainty brought by d59, the value of its possible load fluctuation has become higher, so the fluctuation credit to d119 increases. In Fig. 6(b), while the fluctuation credit to d119 increases with its rising fluctuation level because its rising fluctuation level can enhance the offset, note that the fluctuation payment from d59 decreases because the rising fluctuation level of d119 can reduce the impact of d59's fluctuation on system balance.

Furthermore, to validate what we have discussed in Remark 1, the fluctuation payment from loads and the net revenue of the SO under the ex-ante scheme in (22) were compared with that under the ex-post scheme in (25), with the following steps:

(i) We generated 500 Monte Carlo Samples based on the occurrence probabilities of non-base scenarios in Table VII;

(ii) We calculated the fluctuation payment in each Monte Carlo Sample under the ex-post scheme, and presented it with the red curve in Fig. 7(a). At the same time, under the ex-ante scheme, the fluctuation payment is fixed at $1081.67 in all Monte Carlo Samples, and we presented it with the blue curve in Fig. 7(a);

(iii) We calculated the net revenue of the SO in each Monte Carlo Sample under the ex-post scheme, and we presented it with the red curve in Fig. 7(b). At the same time, under the ex-ante scheme, we calculated the net revenue of the SO in each Monte Carlo Sample and presented it with the blue curve in Fig. 7(b);

(iv) We calculated the average accumulated net revenue of the SO under the ex-post scheme among different numbers of Monte Carlo samples from 1, 2,... to 500, and we presented it with the red curve in Fig. 7(c). At the same time, under the ex-ante scheme, we calculated the average accumulated net revenue of the SO and presented it with the blue curve in

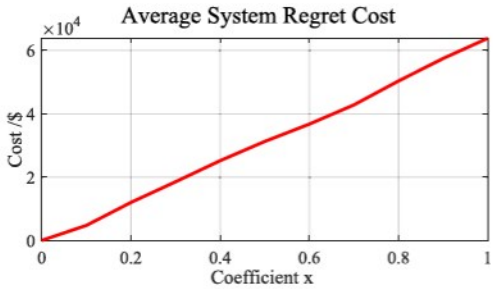

Fig. 8. Average System Regret Cost with respect to the Increasing Occurrence Probabilities of Unforeseen Non-base Scenarios (Increasing Value of Coefficient x).

Fig. 7(c). It can be observed that under the ex-ante scheme, the fluctuation payment from loads is fixed at \$1081.67. On the contrary, under the ex-post scheme, the fluctuation payment from loads is extremely high in some Monte Carlo Samples where one of the extreme scenario happens. For example, in the 151^{st} Monte Carlo Sample, the fluctuation payment under the ex-post scheme is \$43178.64, which is about 40 times as much as the fluctuation payment under the ex-ante scheme. This reveals the financial risk of consumers under the ex-post scheme. In addition, from Fig. 7(b), it can be observed that under the ex-ante scheme, the net revenue of the SO is very closed to zero in most Monte Carlo Samples. On the contrary, under the ex-post scheme, the net revenue of the SO is negative in most Monte Carlo Samples. In those Monte Carlo Samples where one of the extreme scenario happens and the fluctuation payment is large, the SO earns much money. This reveals the financial risk of the SO under the ex-post scheme. Moreover, from Fig. 7(c), it can be observed that with the increasing number of Monte Carlo Samples, the average accumulated net revenue of the SO converges to 0 under both the ex-ante scheme and the ex-post scheme, but the convergence speed under the ex-ante scheme is faster.

Furthermore, considering more numbers of Monte Carlo samples, i.e., 50000, the average accumulated net revenue of the SO under the ex-ante scheme is \$6.00, which is extremely small considering the expected system total cost of this modified 118-bus case \$89648.5. Therefore, we can further confirm the property of revenue adequacy.

On top of that, to make the proposed method more general, here we relaxed assumption (v) and tested the system regret cost of the proposed model (II) with imperfect probability forecasts. Namely, we assumed there were 2 unforeseen non-base scenarios with the outage of the biggest online generator G30: unforeseen non-base scenario I with the outage of G30 and the base load; unforeseen non-base scenario II with the outage of G30 and all loads increased by 2%. The occurrence probabilities of unforeseen scenarios I and II were set as $0.08*$x and $0.01*$x, respectively, parameterized by a non-negative coefficient x: zero value of x means that the forecast of non-base scenarios is accurate, while a positive value of x means that the forecast deviates from the true probability information. And a higher value of x means that the forecast deviates farther from the true probability information. In that sense, in Fig. 8, with the Monte Carlo Simulation, the average system regret costs under different values of x were calculated, with the following steps:

(i) We selected some different values of x between 0 and 1;

(ii) For each value of x, We generated 5000 Monte Carlo Samples based on the occurrence probabilities of foreseen non-base scenarios in Table VII and the occurrence probabilities of unforeseen scenarios ($0.08*$x,$0.01*$x) with given x;

(iii) For each value of x, we calculated the corresponding average system regret cost as the average system revenue deficit in corresponding 5000 Monte Carlo Samples;

(iv) We presented the average system regret costs under different values of x in Fig. 8 as the red curve. It can be observed that when the value of x is 0, the forecast is accurate and the average system regret cost is very closed to 0. With the increasing coefficient x, the forecast becomes more inaccurate and the average system regret cost becomes higher.

In addition to those in-sample tests above, the out-of-sample test was also performed based on previous publications [25] and [40]. In this case, instead of adopting the setting of non-base scenarios in Table VII, we considered possible variations of six major loads in the system, i.e., d54, d59, d80, d90, d116, and d119, and we assumed other loads to be constant. With such settings, load power uncertainty in the system could be properly approximated by countable scenarios. The forecast errors of these variational loads were modelled using several independent Gaussian distributions $\mathcal{N}(\mu, \Sigma)$. For each of them, the mean μ_l of its distribution $\mathcal{N}_l$ was set to be 0, and the variance Σ_l was set to be $0.01d(l)$, where $d(l)$ was its base-case load power. We also considered possible outages of line 21, line 55 and line 102, and we modelled them using several independent Bernoulli distributions. For each of them, its outage followed an occurrence probability of 0.1. Then based on above probability information, we used the Monte Carlo Simulation method to generate 100000 samples to comprise the entire data pool, and we divided the set of these samples into two parts. One part with 90000 samples was considered as in-sample data and was used to generate 400 representative non-base scenarios to drive the proposed co-optimization. Another part with the remaining 10000 samples was used for the out-of-sample test.

The out-of-sample test for the system cost was performed via a similar process as the in-sample average system cost comparison between the proposed model (II) and the traditional deterministic model (I), with the following steps:

(i) We selected different reserve requirements for the traditional model, and calculated the energy and reserve clearing results and base-case procurement costs with the traditional model under different reserve requirement settings;

(ii) We calculated the average re-adjustment costs of the traditional model under different reserve requirement settings for all samples in the out-of-sample set. If the re-adjustment problem was infeasible in any sample, then the re-adjustment cost for that sample was set as 200000.

(iii) We obtained the average system costs of the traditional deterministic model under different reserve requirement settings by adding the base-case procurement costs from step (i) to the average re-adjustment costs from step (ii), and we presented them in Fig. 9 as the red curve.

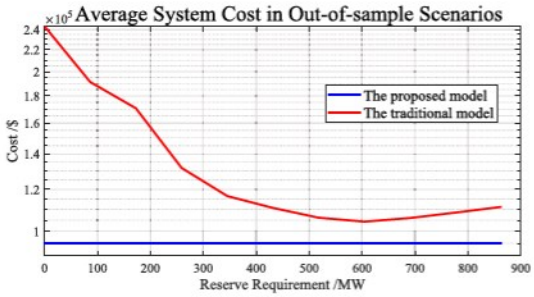

Fig. 9. Average system costs from the proposed model (blue) and the traditional model under different reserve requirement settings (red) in out-of-sample scenarios.

(iv) We calculated the procurement results and base-case procurement costs with the proposed model based on selected representative in-sample scenarios. Then we repeated steps (ii)-(iii) for the proposed model to obtain the average system cost of the proposed model for all samples in the out-of-sample set, and we presented the result in Fig. 9 as the blue curve. We can observe that in the out-of-sample test, the proposed model could still efficiently reduce the average system cost compared with the traditional model, similar as the result from the in-sample test in Fig. 4.

VII. Conclusion

Traditional energy-reserve co-optimization highly relies on empirical reserve zones and zonal reserve requirements. In this paper, a scenario-oriented energy-reserve co-optimization model has been developed, considering congestions and re-adjustment costs of all non-base scenarios. As a result, reserve resources can be optimally procured system-wide to guard against possible contingencies and load/renewable fluctuations.

In addition, prices of energy and reserve have been derived based on their marginal costs/benefits to the joint clearing of energy and reserve. A key question is that should energy, reserve, and re-dispatch at the same bus be considered as homogeneous goods. If they are, under given assumptions, they will be settled at uniform prices. We have also established properties of cost recovery for generators and revenue adequacy for the system operator.

In future studies, more efforts will be made to the coupling of reserve and ramping in multi-period operation and the modelling and pricing of generator outages.

Appendix A

Proof of Theorem 2 (Proportional Locational Uniform Pricing for Re-Dispatch)

According to the KKT conditions and ignoring $\overline{\tau}_k^*(l)$, with the Lagrangian of model (II) denoted as $\mathcal{L}_{II}$, we have:

$$\frac{\partial \mathcal{L}_{II}}{\partial \delta d_k(l)} = \epsilon_k c_L(l) - \underline{\tau_k}^*(l) - \lambda_k^* + S_{D,k}(\cdot, m_l)^{\mathrm{T}} \mu_k^* = 0, \tag{45}$$

$$\frac{\partial \mathcal{L}_{II}}{\partial \delta g_k^U(j)} = \epsilon_k \overline{c}(j) - \underline{\alpha_k}^*(j) + \overline{\alpha_k}^*(j) - \lambda_k^* + S_{G,k}(\cdot, m_j)^{\mathrm{T}} \mu_k^* = 0, \tag{46}$$

$$\frac{\partial \mathcal{L}_{II}}{\partial \delta g_k^D(j)} = -\epsilon_k \underline{c}(j) - \underline{\beta_k}^*(j) + \overline{\beta_k}^*(j) + \lambda_k^* - S_{G,k}(\cdot, m_j)^{\mathrm{T}} \mu_k^* = 0. \tag{47}$$

With $\delta d_k(l), \delta g_k^U(j), \delta g_k^D(j)$ respectively multiplied to both the left-hand side and the right-hand side of (45)-(47), combined with the complementary slackness of (11)-(13) we have:

$$\lambda_k^* \delta d_k(l) = \epsilon_k c_L(l) \delta d_k(l) + S_{D,k}(\cdot, m_l)^{\mathrm{T}} \mu_k^* \delta d_k(l), \tag{48}$$

$$\overline{\alpha_k}^*(j) r_U(j) = -\epsilon_k \overline{c}(j) \delta g_k^U(j) + (\lambda_k^* - S_{G,k}(\cdot, m_j)^{\mathrm{T}} \mu_k^*) \delta g_k^U(j), \tag{49}$$

$$\overline{\beta_k}^*(j) r_D(j) = \epsilon_k \underline{c}(j) \delta g_k^D(j) + (S_{G,k}(\cdot, m_j)^{\mathrm{T}} \mu_k^* - \lambda_k^*) \delta g_k^D(j). \tag{50}$$

With (49), for generator j we have:

$$\Pi_k^U(j) = \overline{\alpha_k}^*(j) r_U(j) + \epsilon_k \overline{c}(j) \delta g_k^U(j) = \omega_k(m_j) \delta g_k^U(j). \tag{51}$$

Similarly, for generator i we have:

$$\Pi_k^U(i) = \omega_k(m_i) \delta g_k^U(i). \tag{52}$$

In addition, apparently we know that $\omega_k(m_i) = \omega_k(m_j)$, then along with (51)-(52), we can prove Theorem 2.

Appendix B

Proof of Theorem 3 (Individual Rationality)

We present the Lagrangian of the proposed model (II) in (53). Furthermore, the Lagrangian of the profit maximization model (IV) of each generator j is

$$\begin{aligned}\mathcal{L}_{IV} = &-\eta^g(j) \times g(j) - \eta^U(j) \times r_U(j) - \eta^D(j) \times r_D(j) \\ &+ c_g(j) \times g(j) + c_U(j) \times r_U(j) + c_D(j) \times r_D(j) \\ &+ \overline{v}(j)(g(j) + r_U(j) - \overline{G}(j)) + \underline{v}(j)(r_D(j) - g(j)) \\ &+ \underline{\rho^U}(j)(0 - r_U(j)) + \overline{\rho^U}(j)(r_U(j) - \overline{r_U}(j)) \\ &+ \underline{\rho^D}(j)(0 - r_D(j)) + \overline{\rho^D}(j)(r_D(j) - \overline{r_D}(j)).\end{aligned} \tag{54}$$

With the formulations of $(\eta^g(j), \eta^U(j), \eta^D(j))$ in (14), (16) and (17), we can observe that the Lagrangian of model (IV) in (54) is a part of the Lagrangian of model (II) in (53). Since these two models are both LP models, according to the KKT conditions we can conclude that, for each generator j, its optimal energy and reserve procurement $g^*(j), r_U^*(j), r_D^*(j)$ solved from model (II) is also the solution to its profit maximization model (IV), which proves Theorem 3.

APPENDIX C
PROOF OF THEOREM 4 (REVENUE ADEQUACY)

To prove revenue adequacy, the phase angle-based form of the proposed co-optimization model is presented as follows:

$$(\mathrm{V}): \quad \underset{\{g,r_U,r_D,\delta g_k^U,\delta g_k^D,\delta d_k,\theta,\theta_k\}}{\text{minimize}} \quad F^V(\cdot),$$

subject to

$$(7),(8),(11),(12),(13),$$

$$\Lambda: A_G \cdot g - A_D \cdot d = B\theta, \tag{55}$$

$$\mu: F\theta \le f, \tag{56}$$

for all $k \in \mathcal{K}$:

$$\Lambda_k: A_G(g + \delta g_k^U - \delta g_k^D) - A_D(d + \pi_k - \delta d_k) = B_k\theta_k, \tag{57}$$

$$\mu_k: F_k\theta_k \le f_k, \tag{58}$$

where $F^V(\cdot)$ represents the objective function of the phase angle-based model (V), which is the same as $F^{II}(\cdot)$ in the shift factor-based model (II). A_G and A_D are matrices that connect generators and loads with nodes, respectively. Vectors θ and θ_k are the phase angle vectors in the base case and in scenario k, respectively. Matrices B and B_k denote the coefficient matrices of DC power flow equations in the base case and in scenario k, respectively. Matrices F and F_k are the branch-node admittance matrices in the base case and in scenario k, respectively. With the equivalence of the shift factor-based model (II) and the phase angle-based model (V), for loads we have

$$A_D^{\mathrm{T}}\Lambda = \lambda^* \cdot \mathbb{1}_{ND\times 1} - S_D^{\mathrm{T}}\mu^*, A_D^{\mathrm{T}}\Lambda_k = \lambda_k^* \cdot \mathbb{1}_{ND\times 1} - S_{D,k}^{\mathrm{T}}\mu_k^*, \tag{59}$$

and for generators we have

$$A_G^{\mathrm{T}}\Lambda = \lambda^* \cdot \mathbb{1}_{NG\times 1} - S_G^{\mathrm{T}}\mu^*, A_G^{\mathrm{T}}\Lambda_k = \lambda_k^* \cdot \mathbb{1}_{NG\times 1} - S_{G,k}^{\mathrm{T}}\mu_k^*, \tag{60}$$

Where ND and NG are the numbers of loads and generators, respectively. In addition, we denote the Lagrangian of model (V) as $\mathcal{L}_V$, with the KKT conditions we have:

$$\theta^{\mathrm{T}}\frac{\partial \mathcal{L}_V}{\partial \theta} = (B\theta)^{\mathrm{T}}\Lambda^* + (F\theta)^{\mathrm{T}}\mu^* = 0, \tag{61}$$

$$\theta_k^{\mathrm{T}}\frac{\partial \mathcal{L}_V}{\partial \theta_k} = (B_k\theta_k)^{\mathrm{T}}\Lambda_k^* + (F_k\theta_k)^{\mathrm{T}}\mu_k^* = 0. \tag{62}$$

In addition, for the base case we have:

$$\Gamma_0^d - \Gamma_0^g = (\lambda^* \cdot \mathbb{1}_{ND\times 1} - S_D^{\mathrm{T}}\mu^*)^{\mathrm{T}}d - (\lambda^* \cdot \mathbb{1}_{NG\times 1} - S_G^{\mathrm{T}}\mu^*)^{\mathrm{T}}g \tag{63}$$

and $(f^{\mathrm{T}}\mu = \Delta_0)$. To Consider revenue adequacy for the base case, we have:

$$\begin{aligned}
&(\lambda^* \cdot \mathbb{1}_{ND\times 1} - S_D^{\mathrm{T}}\mu^*)^{\mathrm{T}}d - (\lambda^* \cdot \mathbb{1}_{NG\times 1} - S_G^{\mathrm{T}}\mu^*)^{\mathrm{T}}g \\
&= (A_D^{\mathrm{T}}\Lambda^*)^{\mathrm{T}}d - (A_G^{\mathrm{T}}\Lambda^*)^{\mathrm{T}}g \\
&= (\Lambda^*)^{\mathrm{T}}(B\theta) = (F\theta)^{\mathrm{T}}\mu^* = f^{\mathrm{T}}\mu^*.
\end{aligned} \tag{64}$$

These four equations are based on equations (59)-(60), the complementary slackness of (55), equation (61), and the complementary slackness of (56), respectively. With above equations, we have

$$\Gamma_0^d = \Gamma_0^g + \Delta_0, \tag{65}$$

which proves *revenue adequacy for the base case*.

In addition, the congestion rent contributed from any non-base scenario k $(\Delta_k = f_k^{\mathrm{T}}\mu_k^*)$ is:

$$\begin{aligned}
&f_k^{\mathrm{T}}\mu_k^* = (F_k\theta_k)^{\mathrm{T}}\mu_k^* = -(B_k\theta_k)^{\mathrm{T}}\Lambda_k^* \\
&= (A_D^{\mathrm{T}}\Lambda_k^*)^{\mathrm{T}}(d + \pi_k - \delta d_k) - (A_G^{\mathrm{T}}\Lambda_k^*)^{\mathrm{T}}(g + \delta g_k^U - \delta g_k^D) \\
&= (\lambda_k^* \cdot \mathbb{1}_{ND\times 1} - S_{D,k}^{\mathrm{T}}\mu_k^*)^{\mathrm{T}}(d + \pi_k - \delta d_k) \\
&\quad - (\lambda_k^* \cdot \mathbb{1}_{NG\times 1} - S_{G,k}^{\mathrm{T}}\mu_k^*)^{\mathrm{T}}(g + \delta g_k^U - \delta g_k^D) \\
&= (-S_{D,k}^{\mathrm{T}}\mu_k^*)^{\mathrm{T}}(d + \pi_k - \delta d_k) - (-S_{G,k}^{\mathrm{T}}\mu_k^*)^{\mathrm{T}}(g + \delta g_k^U - \delta g_k^D) \\
&= (-S_{D,k}^{\mathrm{T}}\mu_k^*)^{\mathrm{T}}(d + \pi_k) + (S_{D,k}^{\mathrm{T}}\mu_k^*)^{\mathrm{T}}\delta d_k + (S_{G,k}^{\mathrm{T}}\mu_k^*)^{\mathrm{T}}g \\
&\quad + (S_{G,k}^{\mathrm{T}}\mu_k^*)^{\mathrm{T}}\delta g_k^U - (S_{G,k}^{\mathrm{T}}\mu_k^*)^{\mathrm{T}}\delta g_k^D.
\end{aligned} \tag{66}$$

These six equations are based on the complementary slackness of (58), equation (62), the complementary slackness of (57), equations (59)-(60), the complementary slackness of (9), and some reorganizations, respectively. On top of that, with the complementary slackness of (9) we have:

$$\sum_j \lambda_k^*(g(j) + \delta g_k^U(j) - \delta g_k^D(j)) = \sum_l \lambda_k^*(d(l) + \pi_k(l) - \delta d_k(l)). \tag{67}$$

Moreover, with equation (48) we have:

$$\begin{aligned}
\mathcal{L}_{II}(\cdot) = {} & c_g^{\mathrm{T}}g + c_U^{\mathrm{T}}r_U + c_D^{\mathrm{T}}r_D + \sum_{k\in\mathcal{K}} \epsilon_k(\overline{c}^{\mathrm{T}}\delta g_k^U - \underline{c}^{\mathrm{T}}\delta g_k^D + c_d^{\mathrm{T}}\delta d_k + \lambda\left(\sum d - \sum g\right) + \mu(S_G^{\mathrm{T}}g - S_D^{\mathrm{T}}d - f) \\
& + \overline{v}(g + r_U - \overline{G}) + \underline{v}(\underline{G} + r_D - g) + \underline{\rho^U}(0 - r_U) + \overline{\rho^U}(r_U - \overline{r_U}) + \underline{\rho^D}(0 - r_D) + \overline{\rho^D}(r_D - \overline{r_D}) + \sum_{k\in\mathcal{K}} \underline{\alpha_k}(0 - \delta g_k^U) \\
& + \sum_{k\in\mathcal{K}} \overline{\alpha_k}(\delta g_k^U - r_U) + \sum_{k\in\mathcal{K}} \lambda_k\left(\sum(d + \pi_k - \delta d_k) - \sum\left(g + \delta g_k^U - \delta g_k^D\right)\right) + \sum_{k\in\mathcal{K}} \underline{\tau_k}(0 - \delta d_k) + \sum_{k\in\mathcal{K}} \overline{\tau_k}(\delta d_k - d - \pi_k) \\
& + \sum_{k\in\mathcal{K}} \overline{\beta_k}(\delta g_k^D - r_D) + \sum_{k\in\mathcal{K}} \underline{\beta_k}(0 - \delta g_k^D) + \sum_{k\in\mathcal{K}} \mu_k(S_{G,k}^{\mathrm{T}}((g + \delta g_k^U - \delta g_k^D) - S_{D,k}^{\mathrm{T}}(d + \pi_k - \delta d_k)) - f_k).
\end{aligned} \tag{53}$$

$$\sum_l \lambda_k^*(d(l)+\pi_k(l)-\delta d_k(l))$$
$$=\sum_l(\lambda_k^* d(l)+\lambda_k^*\pi_k(l)-\epsilon_k c_L(j)\delta d_k(l)-S_{D,k}(\cdot,m_l)^{\mathrm{T}}\mu_k^*\delta d_k(l)), \tag{68}$$

which can be reorganized according to (49)-(50) and (67) as

$$\sum_l(\lambda_k^*(d(l)+\pi_k(l))-(\epsilon_k c_L(l)+S_{D,k}(\cdot,m_l)^{\mathrm{T}}\mu_k^*)\delta d_k(l)$$
$$-\sum_j \lambda_k^* g(j)$$
$$=\sum_j(\overline{\alpha}_k^*(j)r_U(j)+\epsilon_k\overline{c}(j)\delta g_k^U(j)+S_{G,k}(\cdot,m_j)^{\mathrm{T}}\mu_k^*\delta g_k^U(j))$$
$$-\sum_j(-\overline{\beta}_k^*(j)r_D(j)+\epsilon_k\underline{c}(j)\delta g_k^D(j)+S_{G,k}(\cdot,m_j)^{\mathrm{T}}\mu_k^*\delta g_k^D(j)). \tag{69}$$

If we add term $(\sum_l S_{D,k}(\cdot,m_l)^{\mathrm{T}}\mu_k^*(d(l)+\pi_k(l))+\sum_j S_{G,k}(\cdot,m_j)^{\mathrm{T}}\mu_k^* g(j))$ and its opposite to the right-hand side of (69) and reorganize the equation, we have:

$$\sum_l(\lambda_k^*-S_{D,k}(\cdot,m_l)^{\mathrm{T}}\mu_k^*)(d(l)+\pi_k(l))$$
$$=\sum_j(\lambda_k^* g(j)-S_{G,k}(\cdot,m_j)^{\mathrm{T}}\mu_k^* g(j))$$
$$+\sum_j\overline{\alpha}_k^*(j)r_U(j)+\sum_j\overline{\beta}_k^*(j)r_D(j)$$
$$+\sum_j\epsilon_k\overline{c}(j)\delta g_k^U(j)-\sum_j\epsilon_k\underline{c}(j)\delta g_k^D(j)+\sum_l\epsilon_k c_L(l)\delta d_k(l)$$
$$+\left(\sum_j S_{G,k}(\cdot,m_j)^{\mathrm{T}}\mu_k^* g(j)+\sum_j S_{G,k}(\cdot,m_j)^{\mathrm{T}}\mu_k^*\delta g_k^U(j)\right.$$
$$\left.-\sum_j S_{G,k}(\cdot,m_j)^{\mathrm{T}}\mu_k^*\delta g_k^D(j)+\sum_l S_{D,k}(\cdot,m_l)^{\mathrm{T}}\mu_k^*\delta d_k(l)\right)$$
$$-\sum_l S_{D,k}(\cdot,m_l)^{\mathrm{T}}\mu_k^*(d(l)+\pi_k(l)). \tag{70}$$

The term on the left-hand side of (70) is the contribution of scenario k to load payment, including energy payment (21) and load fluctuation payment (22). The right-hand side of equation (70) include the contribution of scenario k to energy credit (19) in the 1^{st} row, its contribution to upward and downward reserve credit (23)-(24) in the 2^{nd} row, its contribution to expected re-dispatch payment (26)-(27) and expected load shedding compensation (28) in the 3^{rd} row, and its contribution to congestion rent in the 4^{th}-6^{th} rows. Therefore, equation (70) can prove *revenue adequacy for any scenario* k. Along with *revenue adequacy for the base case* in (65), we can prove Theorem 4.

APPENDIX D
MULTI-PERIOD EXTENSION OF THE PROPOSED MODEL

$$F^{VI}(g_t,r_{U,t},r_{D,t},\delta g_{k,t}^U,\delta g_{k,t}^D,\delta d_{k,t}) \tag{71}$$
$$=\sum_{t\in T}\Big(c_g^{\mathrm{T}}g_t+c_U^{\mathrm{T}}r_{U,t}+c_D^{\mathrm{T}}r_{D,t}$$
$$+\sum_{k\in\mathcal{K}}\epsilon_k(\overline{c}^{\mathrm{T}}\delta g_{k,t}^U-\underline{c}^{\mathrm{T}}\delta g_{k,t}^D+c_L^{\mathrm{T}}\delta d_{k,t})\Big),$$

$$\text{(VI)}: \underset{\{g_t,r_{U,t},r_{D,t},\delta g_{k,t}^U,\delta g_{k,t}^D,\delta d_{k,t}\}}{\text{minimize}} F^{VI}(\cdot),$$

subject to for all $t\in T$:

$$\lambda_t,: \mathbb{1}^{\mathrm{T}}g_t=\mathbb{1}^{\mathrm{T}}d_t, \tag{72}$$
$$\mu_t: S_{G,t}\cdot g_t-S_{D,t}\cdot d_t\le f_t, \tag{73}$$
$$(\underline{v_t},\overline{v_t}): \underline{G}+r_{D,t}\le g_t, g_t+r_{U,t}\le\overline{G}, \tag{74}$$
$$(\underline{\rho_t^U},\overline{\rho_t^U},\underline{\rho_t^D},\overline{\rho_t^D}): 0\le r_{U,t}\le\overline{r_U}, 0\le r_{D,t}\le\overline{r_D}, \tag{75}$$
$$\gamma_t^U: g_t-g_{t-1}+r_{U,t-1}\le\Delta g^U, \tag{76}$$
$$\gamma_t^D: -g_t+g_{t-1}+r_{D,t-1}\le\Delta g^D, \tag{77}$$

for all $k\in\mathcal{K}$:

$$\lambda_{k,t}: \mathbb{1}^{\mathrm{T}}(g_t+\delta g_{k,t}^U-\delta g_{k,t}^D)=\mathbb{1}^{\mathrm{T}}(d_t+\pi_{k,t}-\delta d_{k,t}), \tag{78}$$
$$\mu_{k,t}: S_{G,kt}(g_t+\delta g_{k,t}^U-\delta g_{k,t}^D)-S_{D,kt}(d_t+\pi_{k,t}-\delta d_{k,t})\le f_k, \tag{79}$$
$$(\underline{\alpha_{k,t}},\overline{\alpha_{k,t}}): 0\le\delta g_{k,t}^U\le r_{U,t}, \tag{80}$$
$$(\underline{\beta_{k,t}},\overline{\beta_{k,t}}): 0\le\delta g_{k,t}^D\le r_{D,t}, \tag{81}$$
$$(\underline{\tau_{k,t}},\overline{\tau_{k,t}}): 0\le\delta d_{k,t}\le d_t+\pi_{k,t}, \tag{82}$$

which gives the multi-period extension of model (II).

REFERENCES

[1] J. Shi, Y. Guo, L. Tong, W. Wu, and H. Sun, "A scenario-oriented approach for energy-reserve joint procurement and pricing," in *Proc. IEEE Power Energy Soc. Gen. Meeting*, 2021, pp. 1–5.

[2] Our World in Data, "Installed solar energy capacity." Jul. 2021. Accessed: Sep. 14, 2021. [Online]. Available: https://ourworldindata.org/grapher/installed-solar-pv-capacity

[3] Our World in Data, "Installed wind energy capacity," Jul. 2021. Accessed: Sep. 15, 2021. [Online]. Available: https://ourworldindata.org/grapher/cumulative-installed-wind-energy-capacity-gigawatts

[4] J. Ellison, V. Loose, and L. Tesfatsion, "A survey of operating reserve markets in U.S. ISO/RTO-managed electric energy regions," Albuquerque, NM, Livermore, CA, USA: Sandia Natl Labs Publications, Rep. SAND2012-1000, Jan. 2012.

[5] Z. Zhou, T. Levin, and G. Conzelmann, *Survey of U.S. Ancillary Services Markets*. Argonne, IL, USA: Argonne Natl Labs Publications, 2016.

[6] B. Carlson, Y. Chen, M. Hong, and R. Jones, "Miso unlocks billions in savings through the application of operations research for energy and ancillary services markets," *INFORMS J. Appl. Analytics*, vol. 42, no. 1, pp. 58–73, 2012.
[7] PJM, "Manual 11: Energy & ancillary services market operations," Oct. 2020. Accessed: Dec. 17, 2020. [Online]. Available: https://www.pjm.com//media/documents/manuals/m11.ashx
[8] CAISO, "2019 annual report on market issues and performance," Jun. 2020. Accessed: Feb. 27, 2021. [Online]. Available: http://www.caiso.com/Documents/2019AnnualReportonMarketIssuesandPerformance.pdf
[9] ISO-NE, "ISO new England manual for forward reserve and real-time reserve," Oct. 2018. Accessed: Mar. 27, 2021. [Online]. Available: https://www.iso-ne.com/static-assets/documents/2018/10/manual_36_forward_reserve_and_realtime_reserve_rev22_20181004.pdf
[10] D. Gezer, A. Nadar, C. Şahin, and N. Özay, "Determination of operating reserve requirements considering geographical distribution of wind power plants," in *Proc. Int. Conf. Clean Elect. Power*, 2011, pp. 797–801.
[11] F. Partovi, B. Mozafari, and M. Ranjbar, "An approach for daily assessment of active power reserve capacity and spinning reserve allocation in a power system," in *Proc. Int. Conf. Power Syst. Technol.*, 2010, pp. 1–8.
[12] M. Bucksteeg, L. Niesen, and C. Weber, "Impacts of dynamic probabilistic reserve sizing techniques on reserve requirements and system costs," *IEEE Trans. Sustain. Energy*, vol. 7, no. 4, pp. 1408–1420, Oct. 2016.
[13] M. A. Matos and R. J. Bessa, "Setting the operating reserve using probabilistic wind power forecasts," *IEEE Trans. Power Syst.*, vol. 26, no. 2, pp. 594–603, May 2011.
[14] J. Saez-Gallego, J. M. Morales, H. Madsen, and T. Jónsson, "Determining reserve requirements in DK1 area of nord pool using a probabilistic approach," *Energy*, vol. 74, pp. 682–693, 2014.
[15] A. Papavasiliou, S. S. Oren, and R. P. O'Neill, "Reserve requirements for wind power integration: A scenario-based stochastic programming framework," *IEEE Trans. Power Syst.*, vol. 26, no. 4, pp. 2197–2206, Nov. 2011.
[16] F. Wang and K. W. Hedman, "Reserve zone determination based on statistical clustering methods," in *Proc. North Amer. Power Symp.*, 2012, pp. 1–6.
[17] F. Wang and K. W. Hedman, "Dynamic reserve zones for day-ahead unit commitment with renewable resources," *IEEE Trans. Power Syst.*, vol. 30, no. 2, pp. 612–620, Mar. 2015.
[18] F. Liu, Z. Bie, C. Wang, and T. Ding, "Energy-reserve co-optimization for energy internet considering reserve control zone determination," in *Proc. IEEE Int. Conf. Energy Internet*, 2017, pp. 83–88.
[19] J. D. Lyon, M. Zhang, and K. W. Hedman, "Locational reserve disqualification for distinct scenarios," *IEEE Trans. Power Syst.*, vol. 30, no. 1, pp. 357–364, Jan. 2015.
[20] H. Ye, Y. Ge, M. Shahidehpour, and Z. Li, "Uncertainty marginal price, transmission reserve, and day-ahead market clearing with robust unit commitment," *IEEE Trans. Power Syst.*, vol. 32, no. 3, pp. 1782–1795, May 2017.
[21] Y. Dvorkin, "A chance-constrained stochastic electricity market," *IEEE Trans. Power Syst.*, vol. 35, no. 4, pp. 2993–3003, Jul. 2020.
[22] G. Pritchard, G. Zakeri, and A. Philpott, "A single-settlement, energy-only electric power market for unpredictable and intermittent participants," *Oper. Res.*, vol. 58, pp. 1210–1219, 2010.
[23] J. M. Morales, A. J. Conejo, K. Liu, and J. Zhong, "Pricing electricity in pools with wind producers," *IEEE Trans. Power Syst.*, vol. 27, no. 3, pp. 1366–1376, Aug. 2012.
[24] J. M. Morales, M. Zugno, S. Pineda, and P. Pinson, "Electricity market clearing with improved scheduling of stochastic production," *Eur. J. Oper. Res.*, vol. 235, no. 3, pp. 765–774, 2014.
[25] J. Kazempour, P. Pinson, and B. F. Hobbs, "A stochastic market design with revenue adequacy and cost recovery by scenario: Benefits and costs," *IEEE Trans. Power Syst.*, vol. 33, no. 4, pp. 3531–3545, Jul. 2018.
[26] S. Wong and J. D. Fuller, "Pricing energy and reserves using stochastic optimization in an alternative electricity market," *IEEE Trans. Power Syst.*, vol. 22, no. 2, pp. 631–638, May 2007.
[27] F. D. Galiana, F. Bouffard, and J. M. Arroyo, "Scheduling and pricing of coupled energy and primary, secondary, and tertiary reserves," *Proc. IEEE*, vol. 93, no. 11, pp. 1970–1983, 2005.
[28] J. Wang, M. Shahidehpour, and Z. Li, "Contingency-constrained reserve requirements in joint energy and ancillary services auction," *IEEE Trans. Power Syst.*, vol. 24, no. 3, pp. 1457–1468, Aug. 2009.
[29] J. M. Arroyo and F. D. Galiana, "Energy and reserve pricing in security and network-constrained electricity markets," *IEEE Trans. Power Syst.*, vol. 20, no. 2, pp. 634–643, May 2005.
[30] G. Zhang, E. Ela, and Q. Wang, "Market scheduling and pricing for primary and secondary frequency reserve," *IEEE Trans. Power Syst.*, vol. 34, no. 4, pp. 2914–2924, Jul. 2019.
[31] H. Chen (PJM), "Security constrained economic dispatch (SCED) overview - prepared by Hong Chen (PJM) for AESO," May 2021. Accessed: Jun. 22, 2021. [Online]. Available: https://www.aeso.ca/assets/Uploads/3.3-SCED-Overview-by-PJM.pdf
[32] A. N. Madavan, S. Bose, Y. Guo, and L. Tong, "Risk-sensitive security-constrained economic dispatch via critical region exploration," in *Proc. IEEE Power Energy Soc. Gen. Meeting*, 2019, pp. 1–5.
[33] Y. Guo, S. Bose, and L. Tong, "On robust tie-line scheduling in multi-area power systems," *IEEE Trans. Power Syst.*, vol. 33, no. 4, pp. 4144–4154, Jul. 2018.
[34] ERCOT, "Module 6: Real-time operations," May 2020. Accessed: Sep. 15, 2020. [Online]. Available: https://www.ercot.com/files/docs/2020/05/12/2019_09_Set301_M6_-_RT.pdf
[35] CAISO, "Flexible ramping product: Revised draft final proposal," Dec. 2015. Accessed: Jun. 04, 2021. [Online]. Available: https://www.caiso.com/Documents/RevisedDraftFinalProposal-FlexibleRampingProduct-2015.pdf
[36] J. Shi, Y. Guo, L. Tong, W. Wu, and H. Sun, "A scenario-oriented approach to multi-period energy-reserve joint procurement and pricing," Sep. 2021. Accessed: Sep. 26, 2021. [Online]. Available: https://arxiv.org/pdf/2109.11993.pdf
[37] Y. Guo, C. Chen, and L. Tong, "Pricing multi-interval dispatch under uncertainty Part I: Dispatch-following incentives," *IEEE Trans. Power Syst.*, vol. 36, no. 5, pp. 3865–3877, Sep. 2021.
[38] PJM, "Day-ahead market clearing process." Apr. 2017. Accessed: Jan. 15, 2022. [Online]. Available: https://pjm.com/-/media/committees-groups/committees/mic/20170425-special/20170425-item-02-day-ahead-market-process.ashx
[39] J. Shi, "Modified case118 data," Apr. 2021. Accessed: Apr. 19, 2021. [Online]. Available: https://github.com/TBSI-SJT/modified_case118_data
[40] L. Yang, Y. Xu, H. Sun, and W. Wu, "Tractable convex approximations for distributionally robust joint chance constrained optimal power flow under uncertainties," *IEEE Trans. Power Syst.*, 2021, doi: 10.1109/TPWRS.2021.3115521.

Jiantao Shi (Student Member, IEEE) received the B.S. degree in electrical engineering from the South China University of Technology, Guangzhou, China, in 2019, and the M.S. degree in electrical engineering in 2021 from Tsinghua-Berkeley Shenzhen Institute, Shenzhen International Graduate School, Tsinghua University, Shenzhen, China, where he is currently working toward the Ph.D. degree in electrical engineering. His research interests include power system economics, ancillary service market, and uncertainty pricing. He was the recipient of the Best Paper Award at 2021 IEEE PES General Meeting, Best Industrial Paper Award at 2021 IEEE IAS I&CPS Asia, and Best Paper Award at the 5th IEEE EI2 Conference.

Ye Guo (Senior Member, IEEE) received the B.E. and Ph.D. degrees from the Department of Electrical Engineering, Tsinghua University, Beijing, China, in 2008 and 2013, respectively. He is currently an Associate Professor with Tsinghua-Berkeley Shenzhen Institute, Tsinghua University. From 2014 to 2018, he was a Postdoctoral Associate with Cornell University, Ithaca, NY, USA. His research interests include distributed optimization, game and market theory, state estimation, and their applications in power and energy systems. Between 2019 and 2021, he won the IEEE PES General Meeting Best Paper Award four times in three years in a row, with one coauthored paper being selected as the Best-of-the-Best Papers. He was also the recipient of the Best Poster Award at PSERC IAB Meeting 2018, and Best Paper Award at the 4th IEEE EI2 Conference.

Lang Tong (Fellow, IEEE) received the B.E. degree from Tsinghua University, Beijing, China, in 1985, and the M.S. and Ph.D. degrees in electrical engineering from the University of Notre Dame, Notre Dame, IN, USA, in 1987 and 1991, respectively. He is the Irwin and Joan Jacobs Professor of engineering with Cornell University, Ithaca, NY, USA, and the Site Director of the Power Systems Engineering Research Center. In 1991, he was a Postdoctoral Research Affiliate with the Information Systems Laboratory, Stanford University, Stanford, CA, USA. He was the 2001 Cor Wit Visiting Professor with the Delft University of Technology, Delft, The Netherlands, and held visiting positions with Stanford University, and the University of California at Berkeley, Berkeley, CA, USA. His research interests include statistical inference, communications, and complex networks. His current research focuses on inference, optimization, and economic problems in energy and power systems.

Dr. Tong was a Distinguished Lecturer of the IEEE Signal Processing Society. He was the recipient of the 1993 Outstanding Young Author Award from the IEEE Circuits and Systems Society, 2004 Best Paper Award from IEEE Signal Processing Society, 2004 Leonard G. Abraham Prize Paper Award from the IEEE Communications Society, and Young Investigator Award from the Office of Naval Research. He is also a coauthor of seven student paper awards.

Wenchuan Wu (Fellow, IEEE) received the B.S., M.S., and Ph.D. degrees from the Department of Electrical Engineering, Tsinghua University, Beijing, China. He is currently a Professor with Tsinghua University and the Deputy Director of the State Key Laboratory of Power Systems. His research interests include energy management system, active distribution system operation and control, machine learning, and its application in energy system. Prof. Wu was the recipient of the National Science Fund of China Distinguished Young Scholar Award in 2017.

Hongbin Sun (Fellow, IEEE) received the B.S. and Ph.D. degrees from the Department of Electrical Engineering, Tsinghua University, Beijing, China, in 1992 and 1996, respectively. He is currently the ChangJiang Scholar Chair Professor with the Department of Electrical Engineering and the Director of Energy Management and Control Research Center, Tsinghua University. He has authored or coauthored more than 400 peer-reviewed papers, within which more than 60 are IEEE and IET journal papers, and four books. He has been granted five U.S. Patents of Invention and more than 100 Chinese patents of invention. His technical and research interests include electric power system operation and control and energy system integration. He is an IET Fellow. He is also the Editor of the IEEE TRANSACTIONS ON SMART GRID, an Associate Editor for the *IET Renewable Power Generation*, and a Member of the Editorial Board of four international journals and several Chinese journals.